Strain effects on the behavior of isolated and paired sulfur vacancy defects in monolayer MoS_{2}

Mehmet Gokhan Sensoy, Dmitry Vinichenko, Wei Chen, Cynthia M. Friend, and Efthimios Kaxiras

Phys. Rev. B **95**, 014106 — Published 17 January 2017

DOI: 10.1103/PhysRevB.95.014106

Strain effects on the behavior of isolated and paired sulfur vacancy defects in monolayer MoS_2

Mehmet Gokhan Sensoy,[1,2] Dmitry Vinichenko,[3] Wei Chen,[1,4,5] Cynthia M. Friend,[1,3] and Efthimios Kaxiras[1,4,*]

[1] *John A. Paulson School of Engineering and Applied Sciences, Harvard University, Cambridge, Massachusetts 02138, USA*
[2] *Department of Physics, Middle East Technical University, Ankara, 06800, Turkey*
[3] *Department of Chemistry and Chemical Biology, Harvard University, Cambridge, Massachusetts 02138, USA*
[4] *Department of Physics, Harvard University, Cambridge, Massachusetts 02138, USA*
[5] *ICQD, Hefei National Laboratory for Physical Sciences at Microscale, and Synergetic Innovation Center of Quantum Information and Quantum Physics, University of Science and Technology of China, Hefei, Anhui 230026, China*

(Dated: December 13, 2016)

We investigate the behavior of sulfur vacancy defects, the most abundant type of intrinsic defect in monolayer MoS_2, using first-principles calculations based on density functional theory. We consider the dependence of the isolated defect formation energy on the charge state and on uniaxial tensile and compressive strain up to 5%. We also consider the possibility of defect clustering by examining the formation energies of pairs of vacancies at various relative positions, and their dependence on charge state and strain. We find that there is no driving force for vacancy clustering, independent of strain in the material. The barrier for diffusion of S vacancies is larger than 1.9 eV in both charged and neutral states regardless of the presence of other nearby vacancies. We conclude that the formation of extended defects from S vacancies in planar monolayer MoS_2 is hindered both thermodynamically and kinetically.

PACS numbers: 73.20.Hb, 68.35.Dv, 61.72.J-, 62.20.-x

I. INTRODUCTION

The class of semiconducting, two dimensional (2D) materials referred to as transition metal dichalcogenides (TMDCs) has been the subject of intense research activity due to their interesting behavior which includes their photoluminescence (PL) properties,[1,2] interlayer excitons,[3] and valley physics.[4] The prototypical material in this class, MoS_2, has been studied for potential applications in the context of catalysis,[5–7] in energy storage,[8] and as an electrode for hydrogen evolution.[9–14] Moreover, single layers of this compound have been proposed for use in field-effect transistors,[15–20] including bendable devices[21] and integrated circuits.[22,23] In most of these applications, the defect properties of MoS_2 monolayers are of central importance. In this work, we use first-principles computations to study the sulfur vacancy in MoS_2, which is the intrinsic defect with the lowest formation energy.[24] We investigate the formation energy and diffusion barrier of this defect as a function of charge state and strain, as well as the collective behavior of vacancies, that is, the interactions between vacancy pairs at various distances. These aspects of their behavior may prove important in understanding the nature of the recently proposed ripplocation structure[25].

The paper is organized as follows: in Section II we present the methodology used for the calculations; in Section III we discuss various aspects of the sulfur vacacny defect, including the structural and electronic properties of isolated vacancies (part A), the properties of vacancy pairs in various configurations (part B) and the energy barriers for vacancy diffusion (part C); finally, Section IV contains a short summary and discussion of the implications of our results for the luminescence signature of S vacancy defects in unstrained and strained monolayer MoS_2.

II. METHODOLOGY

Our calculations are based on the plane-wave, pseudopotential density functional theory (DFT) method as implemented in the Quantum Espresso code suite.[26] The calculations were performed using the Projector Augmented Wave (PAW) formalism which describes well the MoS_2 structure [24,27] with the commonly employed exchange-correlation functional developed by Perdew, Burke and Ernzerhof (PBE).[28] We use Γ-point Brillouin Zone sampling, a cut-off energy of 50 Ry for the wavefunction plane-wave expansion and 500 Ry for the density, and a 6×6 (8×8) super-cell for the isolated defect (pairs) calculations with a 16 Å vacuum region separating the periodic images of layers. All defect configurations are relaxed to the point where the calculated forces on atoms do not exceed in magnitude 0.05 eV/Å. The defect formation energy $E_f(q)$ in the thermodynamic limit is obtained from

$$E_f(q) = E^{def}_{\mathrm{DFT}}(q) - E^{st}_{\mathrm{DFT}} + \mu_{\mathrm{S}} n_{\mathrm{S}} + q(E_{\mathrm{VBM}} + E_F) + E_{corr}(q) \quad (1)$$

where $E_{\rm DFT}^{def}(q)$ is the DFT total energy of the layer containing the defects in the charge state q, $E_{\rm DFT}^{st}$ is the DFT total energy of the stoichiometric layer, $\mu_{\rm S}$ the chemical potential of S, $n_{\rm S}$ the number of S vacancies in the simulation cell, $E_{\rm VBM}$ the valence band maximum energy, E_F the Fermi level with respect to the valence band maximum, and $E_{corr}(q)$ the electrostatic correction necessary for the charged states of the defect. For the chemical potential of S we use the DFT calculated energy of the S_8 molecule in the gas phase, which corresponds to 0 K and S-rich conditions. For the computation of $E_{corr}(q)$ we parametrize the dielectric profile of the model slab $\epsilon(z)$ as a piece-wise constant joined by a smoothing error function, with the dielectric constant of the material being $\epsilon_\perp = 6$, $\epsilon_\parallel = 15$ in the directions perpendicular and parallel to the layer, respectively,[29] and we take the effective layer thickness to be 6 Å. We obtain the defect charge distribution, $\rho_d(\vec{r})$, by summing the magnitude of the occupied defect states in the band gap. We emphasize that our approach is different from earlier related works [30–33] in several important ways, the most important being that we parameterize the dielectric profile by minimizing the potential alignment term, and we use unscreened defect charge density. Moreover, our method [34] allows us to treat both bulk 3D and 2D materials on the same footing, as well as to include relaxation of the ions, an important ingredient missing from earlier methods. With this density, we solve for the defect-induced electrostatic potential under periodic boundary conditions, $V_{\rm PBC}(\vec{r})$, from the Poisson equation, $\nabla[\epsilon(z)\nabla V_{\rm PBC}(\vec{r})] = -\rho_d(\vec{r})$, and compute the corresponding defect charge electrostatic energy under periodic boundary conditions, $E_{\rm PBC} = \frac{1}{2}\int V_{\rm PBC}(\vec{r})\rho_d(\vec{r})d\vec{r}$. In order to obtain the electrostatic energy of the isolated charge under open boundary conditions, E_{iso}, we extrapolate $E_{\rm PBC}$ to the limit of an infinite model cell. The correction is then calculated as a difference of those quantities, $E_{corr}(q) = E_{iso} - E_{\rm PBC}$. This approach and its limitations and advantages are discussed in more detail in a forthcoming article.[34]

III. SULFUR VACANCIES IN MOLYBDENUM DISULFIDE

MoS_2 is a semiconductor, with band gap of 1.9 eV in monolayer[35–38] and 1.3 eV in bulk form.[39] The spin-orbit coupling, which is generally a prominent feature in TMDCs and especially those formed by heavy elements, does not have a substantial effect on the electronic structure of the MoS_2 monolayer.[40] Interestingly, the exciton binding energy is strongly enhanced in the monolayer relative to the bulk.[29,41] The Mo atoms are surrounded by trigonal prisms of S atoms. In a localized representation of the electronic states based on Wannier orbitals, the electronic structure of MoS_2 can be described as a combination of directed σ-bonds between Mo and S atoms (Fig. 1), lone pairs on S atoms, pointing outwards, and non-bonding states localized on the Mo atoms. In this picture, the valence bands are spanned by the σ-bonds and the valence band edge is composed of non-bonding states on Mo.[42]

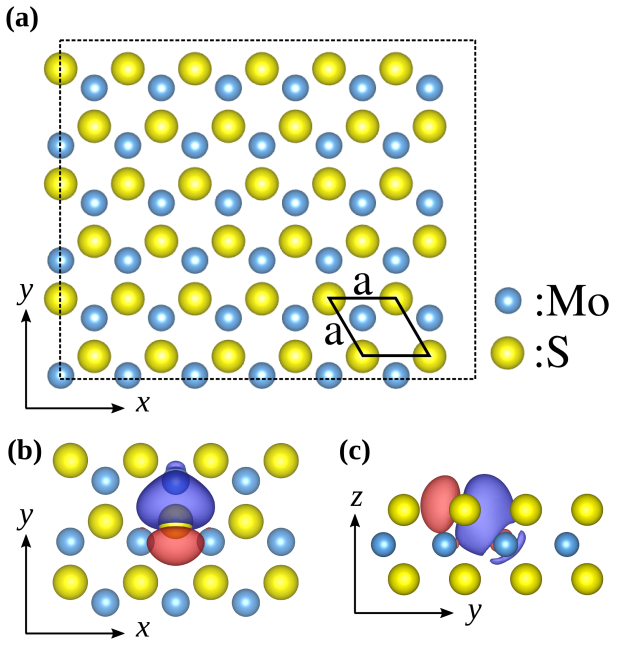

FIG. 1. Top view of square region of the superccell used for the calculations with the primitive unit cell shown in black solid lines, with the lattice constant a=3.195 Å. (b) and (c); top and side views of the neighborhood of the S vacancy defect with the Wannier function corresponding to the σ-bond between the Mo and S atoms. Blue and red lobes are positive and negative isosurfaces of the Wannier function.

The intrinsic defect with the lowest formation energy in monolayer MoS_2 is the S vacancy.[24] Here we consider the neutral ($q = 0$) and charged ($q = -1$) states of S vacancy. We do not consider the charge state $q = -2$ since it was shown to be unstable in previous work.[24]

A. Isolated vacancy

Upon the creation of an isolated S vacancy the relaxation of neighboring atoms is limited to within 4 Å from the vacancy in both the neutral and charged ($q = -1$) states (see Fig. 2(a)). The displacements of atoms farther than 4 Å from the vacancy are smaller than 0.05 Å and are not shown. Two groups of S atoms can be identified depending on their position relative to the vacancy: those that are on the same side of the monolayer with the vacancy, which have larger variance in the displacement ($|\Delta\vec{R}|$) upon relaxation, and those that are on the opposite side of the monolayer from the vacancy, which have smaller displacement. Moreover, the atomic displacements around the vacancy are 10% larger for the charged state compared to neutral state.

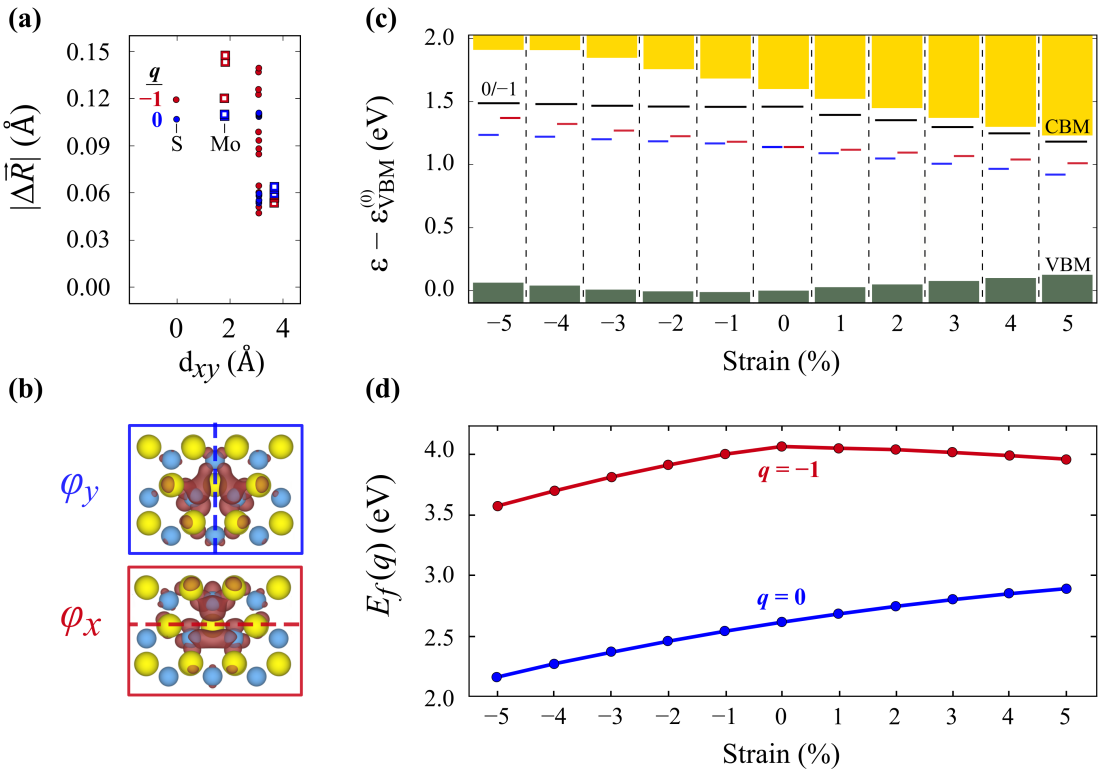

FIG. 2. (a) Magnitude of atomic displacements around the isolated S vacancy in monolayer MoS_2, $|\Delta\vec{R}|$, as a function of distance d_{xy} between the atom and the vacancy in the xy-plane. (b) Isosurfaces of the defect states $|\varphi_x(\vec{r})|^2$ and $|\varphi_y(\vec{r})|^2$; the nodal planes are shown as dashed lines in each case. (c) Energy levels of the defect states φ_y (blue), φ_x (red) and thermodynamic charge transition level (black) in the band gap associated with a single S vacancy: their position within the gap range as a function of uniaxial strain, relative to the valance band maximum of the unstrained monolayer MoS_2, $\varepsilon^{(0)}_{\mathrm{VBM}}$. (d) Formation energy of isolated S vacancy as a function of uniaxial strain.

In order to understand these features, we analyze in detail the electronic structure of the defect. Creation of a S vacancy introduces two unoccupied defect levels in the band gap of the material and one fully occupied state below the valence band maximum. The localized orbitals of the states in the gap originate from the three severed Mo–S σ–bonds and, due to strong overlap between the d-orbitals on Mo atoms, they are delocalized between three Mo atoms adjacent to the vacancy. These localized states can potentially serve as electron traps and affect the exciton binding energy in monolayer MoS_2. Qualitatively, the electronic structure of defect states can be understood by considering ~~a Huckel-type model for~~ the hybrid orbitals of σ-bonds between Mo and S atoms. For three bonds in trigonal arrangement the electronic structure ~~is analogous to the cyclopropene π-system:~~ is described by the following states: one occupied level is resonant with the valence band and two band gap levels are degenerate, with one nodal plane in each of them. The nodal planes are in the xz and yz planes, so the orbitals are labeled φ_x and φ_y, respectively, see Fig. 2(b). Earlier work has shown that the S vacancy can act as an acceptor due to the presence of these empty levels.[24] We investigate how the absolute position of those states in the gap changes under uniaxial strain in the y direction as defined in Fig. 1, the direction that is more susceptible to stretching and is relevant for the possible formation of defects in the recently discovered ripplocation structure[25]. Overall, the band gap of the material decreases with applied tensile strain and increases with compressive strain, in line with previous computational results.[43] Applying strain in the y direction leads to removal of the degeneracy between φ_x and φ_y, with the energy of φ_y being lower than the energy of φ_x, see Fig. 2(c). We hypothesize that this is due to the presence of the nodal plane xz for φ_x, which is perpendicular to the strain direction, so the energy of this state is less affected by the change in the orbital overlap compared to φ_y. Next, we calculate the formation energy of the isolated S vacancy in neutral ($q = 0$) and charged ($q = -1$) states as a function of uniaxial tensile and compressive strain. We have examined this wide range of strain, ±5%, in order to capture the general trends, up to the point where the material actually starts breaking, which is beyond 5%, as indicated by experiment.[44] The formation energy of the defect in the neutral state increases with stretching

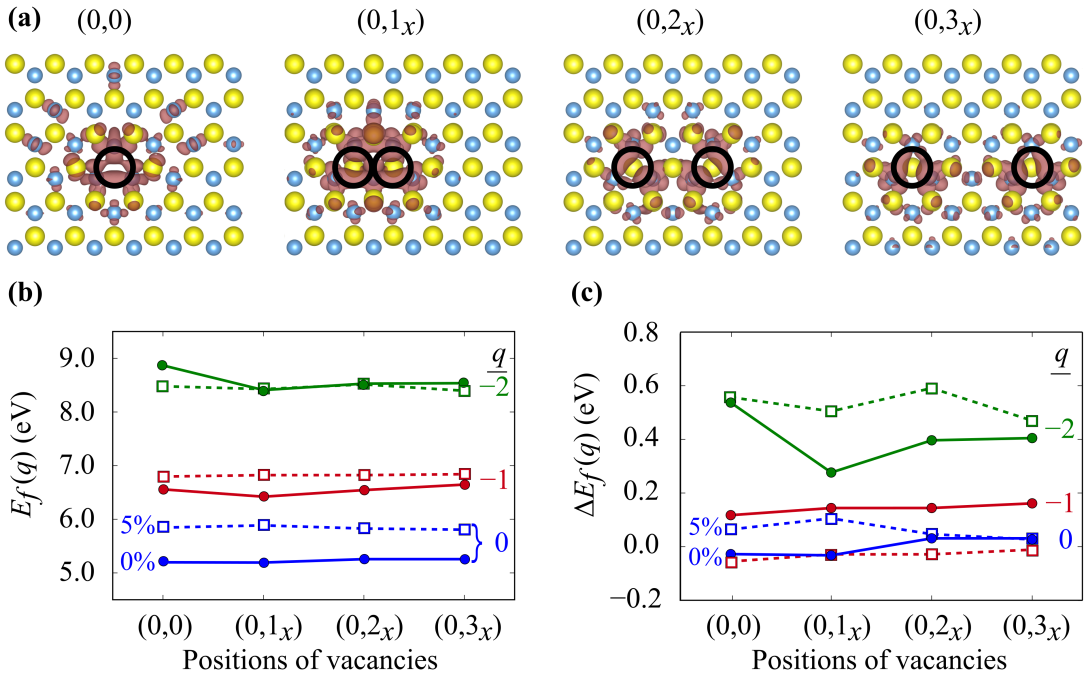

FIG. 3. Clustering of S vacancies. (a) Defect wavefunctions for the pairs of S vacancies in the x direction for various relative positions; black circles highlight the vacancy positions. (b) Formation energies $E_f(q)$ for vacancy pairs in charge states $q = 0, -1, -2$ along the x direction for 0% (solid line, filled circles) and 5% (dashed line, open squares) tensile strain along the y direction. (c) Difference in formation energies of a pair of V_S relative to the energy of two isolated S vacancies, $\Delta E_f(q)$.

the material, which we attribute to the presence of a defect-induced state in the valence band that has bonding character, see Fig. 2(d). For the charged state under compressive strain the behavior is similar to the neutral state. For the tensile strain, the value of the formation energy shows a marginally decreasing dependence on applied strain. We suggest that this effect is due to occupation of the band gap defect level φ_y which is localized on the Mo d-level and has antibonding character, as discussed above. Another factor could be the increase of the occupation of σ^* Mo–S antibonding orbitals surrounding the vacancy through the mechanism of geminal hyperconjugation, which facilitates the lattice relaxation for accommodating the defect, as evidenced by the larger relaxation of the lattice around the charged defect compared to the neutral vacancy, see Fig. 2(a).

We have also considered the transition level, that is, the position of the Fermi level of the material in the gap at which $E_f(0) = E_f(-1)$, denoted by a black line in Fig. 2(c), as a function of strain. We find that this level moves down in energy with increasing tensile strain, while compressive strain does not have a substantial effect on the transition level position. We find that the deep-acceptor character of the isolated S vacancy is preserved throughout the range of strain considered.

B. Vacancy pairs

We address next the possibility of clustering of S vacancies in the MoS_2 monolayer. To this end we calculate the formation energy of two S vacancies as a function of their spatial separation. We consider various configurations of the two vacancies: first on top of each other on opposite sides of the sheet, labeled (0,0), and then, three different cases for vacancies on the same side of the sheet, for both x and y directions: immediately adjacent vacancies labeled (0,1$_x$) and (0,1$_y$), separated by one S atom labeled (0,2$_x$) and (0,2$_y$), and separated by two S atoms labeled (0,3$_x$) and (0,3$_y$). In Fig. 3(a), we show the geometries of vacancy pairs along the x direction. As far as strain is concerned, we compared two cases: unstrained material and 5% tensile strain applied along the y direction. For the neutral vacancies we see virtually no dependence of the formation energy on the relative position of the defects. We attribute this finding to the following effect: due to the two-dimensional nature of the material and its small dielectric constant[45] the relaxation of the atoms around the defect is limited and, as in the isolated vacancy case, the relaxations are localized within 4 Å from the defect, leading to a small value for the elastic component of the defect interaction. Under 5% strain, the neutral vacancy pair formation energy increases almost uniformly by about 0.6 eV for all relative positions of the vacancies, which is very close to twice the 0.3 eV

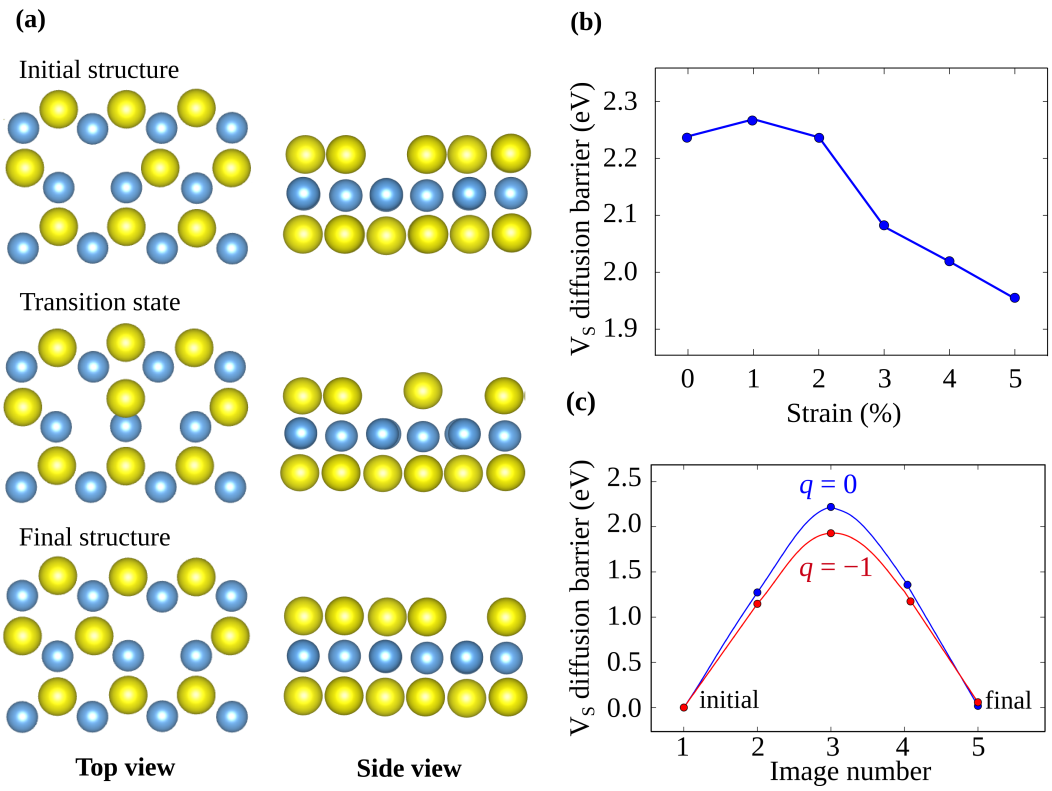

FIG. 4. Energy barriers for S vacancy diffusion: (a) Geometric structures along the NEB path for isolated vacancy in neutral state. (b) Diffusion barrier as a function of strain applied along the y direction. (c) Minimal energy path for the diffusion of an isolated vacancy (solid line) for the neutral (blue, $q = 0$) and charged (red, $q = -1$) states.

increase in formation energy of the isolated vacancy, see Fig. 2(d). From these results we conclude that the elastic interaction between neutral vacancies is negligible. For the case of two charged vacancies ($q = -2$) the formation energies of pairs of vacancies on the same side of the sheet (0, $n_{x/y}$), n = 1, 2, 3 are very close to each other; the formation energy under strain decreases slightly, similar to the isolated vacancy case, see Fig. 2(d). For $q = -1$ there is a slight increase in pair formation energy with strain. Formation energies along the x direction are shown in Fig. 3(b). Formation energies along the y direction (not shown) are very similar to those along the x direction, indicating that the strain-induced anisotropy has negligible effect on vacancy cluster formation. An interesting quantity is the difference of the pair formation energy from the energy of two isolated vacancies, $\Delta E_f(q)$, which is shown in Fig. 3(c). For the neutral ($q = 0$) and charged ($q = -1$) cases the pair formation energy is slightly (up to 0.1 eV) larger than the energy of two isolated vacancies. For $q = -2$, the difference is more pronounced, a fact that we attribute to the higher electrostatic energy of the defect-induced charge. Moreover, the distances between the Mo atoms around the (0,0) vacancy for $q = -2$ are 0.05 Å larger than in the neutral state, consistent with the occupation of defect-induced antibonding levels. In all charge states, the formation energies of pairs in configurations (0,1_x), (0,2_x), (0,3_x) are very close to each other indicating no thermodynamic driving force for the clustering of S vacancies.

C. Diffusion energy barriers

We have also considered the possibility of diffusion of the S vacancies. We use the climbing image nudged elastic band method (CI-NEB)[46] for the computation of the activation energies for diffusion of the S vacancy between adjacent sites. The diffusion pathways in the cases of the isolated and the paired S vacancy are essentially identical, as suggested also by the diffusion energy barriers, so we only discuss the case of the isolated vacancy, see Fig. 4(a). We find that the barrier for isolated vacancy diffusion in the neutral ($q = 0$) state is 2.24 eV, a very large barrier for a thermally activated process. We investigated if the diffusion can be facilitated by other factors, such as applied strain, the presence of other vacancies nearby, or the charge state of the defect. We find that the barrier decreases with applied strain, to 1.95 eV for 5% uniaxial tensile strain, see Fig. 4(b); this result can be rationalized by considering that the strained material can more easily accommodate the lattice relaxation related to defect diffusion. Finally, the diffusion barrier

in the negatively charged ($q = -1$) state is lowered by 0.3 eV compared to the neutral case, for the isolated vacancy, see Fig. 4(c). This result is in line with our previous discussion of charge-induced lattice softening caused by occupation of the antibonding levels in the band gap. Overall, we find that the diffusion of sulfur vacancies is a thermodynamically hindered process, as confirmed by recent experimental work[47] indicating a vacancy jump frequency of 1 per 40 s. Taking into account the absence of a driving force for clustering of the vacancies, we find that the formation of extended defects is an unlikely process barring strong external perturbation, like electron beam irradiation.[47,48]

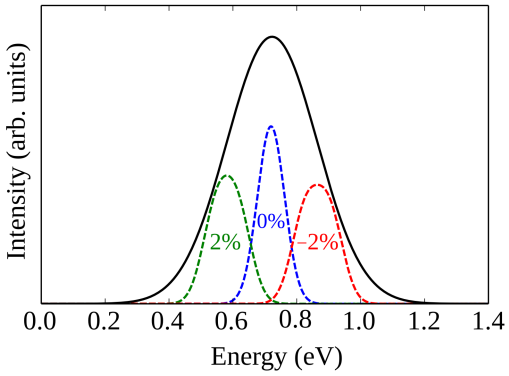

FIG. 5. The expected photoluminescence spectrum peak (black line) from MoS_2 monolayer containing S vacancy defects in regions with no strain (blue dashed line) and regions with -2% (red dashed line) and $+2\%$ (green dashed line); we have assumed a peak width of 60 meV, typical for a free-standing monolayer.

IV. SUMMARY AND DISCUSSION

In summary we have reported a comprehensive examination of the properties of S vacancies, the most prevalent defects in monolayer MoS_2, using first-principles calculations. We find that the formation energy of the neutral S vacancy increases under uniaxial strain in the y direction. For the negatively charged vacancy it decreases under both compressive and tensile strain; we attribute this finding to the fact that defect-induced states in the gap have antibonding character and their occupation leads to lattice softening. Our results also indicate that defect-induced lattice reorganization is very localized and there is no elastic interaction between two adjacent vacancies in either the neutral or the charged state. Accordingly, there is no thermodynamic driving force for the clustering of S vacancies and the barrier for the diffusion of vacancies is high, larger than 1.95 eV, in all cases considered.

It is interesting to examine these findings in the context of the optical properties of exfoliated mineral MoS_2[25] that may contain a large number of vacancy defects, including some in the neighborhood of the ripplocation structure[49]. Firstly, the large formation energy of isolated S vacancies and pairs of vacancies, as well as the large barrier for the diffusion, strongly suggest that such defects are unlikely to form under thermodynamic equilibrium conditions. Secondly, the presence of tensile strain, as is likely the case in large deformations such as the ripplocation, does not change the formation energy or diffusion barrier of neutral S vacancies substantially to alter their equilibrium properties. Therefore, if S vacancies are present they will have to be introduced by external factors, like large forces during exfoliation. Moreover, if vacancies are present, their luminescence properties will be affected by the local strain. Another important factor in the ripplocation geometry can be the bending of the monolayer, which introduces deformation different than the uniform strain considered here; this deserves further detailed consideration.

We will attempt to estimate the energy of the photoluminescence peaks due to the presence of S vacancies from our results so far, even though this cannot be accomplished in a truly quantitative manner because of inherent limitations of the reported calculations. Specifically, we assume that the energy of luminescence peaks is associated with the energy difference between the defect states in the band gap, φ_x and φ_y in the case of the S vacancy, and the conduction band minimum. This assumption means that we are not taking into account excitonic effects, which is beyond the scope of the present work and would require a very different treatment of the electronic states. We will use a strain of $\pm 2\%$ as indicative of values in the exfolitated material with defects, although for specific sites on the ripplocation profile the strain may have even larger values.

In the unstrained material the energy difference between defect-induced gap states and the conduction band minimum is 0.46 eV for the degenerate φ_x and φ_y orbitals, while in the material under 2% tensile strain the energy differences are 0.39, 0.35 eV and under 2% compressive strain they are 0.58, 0.53 eV. The limitation of DFT calculations in reproducing the value of semiconductor band gaps, and by extension the position of defect levels in the the gap, is well established; values for these quantities can be obtained with better accuracy using methodologies like the GW approximation.[50] Typically, the DFT results are off from the more accurate GW results by an overall scaling factor, both for the band gap and for the band width. In order to provide a better estimate for the energy of the photoluminescence peaks associated with S vacancies in the MoS_2 monolayer, we rescale our DFT band gap, which is 1.60 eV, to match the GW band gap[42] which is 2.48 eV. We then use the same scaling factor to determine a reasonable estimate of the position of defect states in the gap, since these are related to orbitals resembling the conduction bands (antibonding states with Mo d-character), as was discussed in Section III A. With this scaling of the energy levels we infer that the approximate positions of defect-induced

photoluminescence peaks would be 0.71 eV for the unstrained material, 0.62 and 0.55 eV under 2% uniaxial tensile strain, and 0.90 and 0.83 eV under 2% compressive strain. Assuming a peak width of 60 meV, typical for a free-standing monolayer, the various contributions would produce a broad photoluminescence peak centered around 0.7 eV. We caution that this can only be viewed as a rough qualitative guide of what may be expected as the signature of the S vacancy presence, and that more accurate results need to be obtained, possibly with the use of time-dependent DFT simulations that can better capture the nature of electronic excitations.

ACKNOWLEDGMENTS

We thank S. N. Shirodkar and R. Kuate Defo for useful discussions and V. Swaminathan for useful comments on the manuscript. MGS acknowledges support from the Scientific and Technological Research Council of Turkey (TUBITAK) 2214-A Program, Grant no. 1059B141500480. DV, EK acknowledge support from ARO MURI W911NF-14-1-0247. DV, CMF acknowledge support from NSF CHE 1362616 Award in the Catalysis program. WC acknowledges support from the National Natural Science Foundation of China Grant No. 11504357. Computational resources were provided by XSEDE (Grant No. TG-DMR120073), which is supported by NSF Grant No. ACI-1053575, and by the FAS Research Computing Group at Harvard University.

AUTHOR CONTRIBUTIONS

MGS and DV contributed equally to this work.

* kaxiras@physics.harvard.edu

[1] T. Cheiwchanchamnangij and W. R. L. Lambrecht, Physical Review B **85**, 205302 (2012).
[2] G. Eda, H. Yamaguchi, D. Voiry, T. Fujita, M. W. Chen, and M. Chhowalla, Nano Letters **11**, 5111 (2011).
[3] P. Rivera, K. L. Seyler, H. Yu, J. R. Schaibley, J. Yan, D. G. Mandrus, W. Yao, and X. Xu, Science **351**, 688 (2016).
[4] A. Kuc, N. Zibouche, and T. Heine, Physical Review B **83**, 245213 (2011).
[5] M. Chhowalla, H. S. Shin, G. Eda, L. J. Li, K. P. Loh, and H. Zhang, Nature Chemistry **5**, 263 (2013).
[6] M. Daage and R. R. Chianelli, Journal of Catalysis **149**, 414 (1994).
[7] W. Chen, E. J. G. Santos, W. Zhu, E. Kaxiras, and Z. Zhang, Nano Letters **13**, 509 (2013).
[8] K. Chang and W. X. Chen, ACS Nano **5**, 4720 (2011).
[9] J. Greeley, T. F. Jaramillo, J. Bonde, I. B. Chorkendorff, and J. K. Norskov, Nature Materials **5**, 909 (2006).
[10] A. B. Laursen, S. Kegnaes, S. Dahl, and I. Chorkendorff, Energy and Environmental Science **5**, 5577 (2012).
[11] T. S. Li and G. L. Galli, Journal of Physical Chemistry C **111**, 16192 (2007).
[12] Y. G. Li, H. L. Wang, L. M. Xie, Y. Y. Liang, G. S. Hong, and H. J. Dai, Journal of the American Chemical Society **133**, 7296 (2011).
[13] D. Merki, S. Fierro, H. Vrubel, and X. L. Hu, Chemical Science **2**, 1262 (2011).
[14] X. Zong, H. J. Yan, G. P. Wu, G. J. Ma, F. Y. Wen, L. Wang, and C. Li, Journal of the American Chemical Society **130**, 7176 (2008).
[15] B. Radisavljevic, A. Radenovic, J. Brivio, V. Giacometti, and A. Kis, Nature Nanotechnology **6**, 147 (2011).
[16] L. T. Liu, S. B. Kumar, Y. Ouyang, and J. Guo, IEEE Transactions on Electron Devices **58**, 3042 (2011).
[17] Y. Yoon, K. Ganapathi, and S. Salahuddin, Nano Letters **11**, 3768 (2011).
[18] Y. J. Zhang, J. T. Ye, Y. Matsuhashi, and Y. Iwasa, Nano Letters **12**, 1136 (2012).
[19] K. Lee, H. Y. Kim, M. Lotya, J. N. Coleman, G. T. Kim, and G. S. Duesberg, Advanced Materials **23**, 4178 (2011).
[20] H.-S. Kim, C.-R. Lee, J.-H. Im, K.-B. Lee, T. Moehl, A. Marchioro, S.-J. Moon, R. Humphry-Baker, J.-H. Yum, J. E. Moser, M. Graetzel, and N.-G. Park, Scientific Reports **2**, 591 (2012).
[21] J. Pu, Y. Yomogida, K. K. Liu, L. J. Li, Y. Iwasa, and T. Takenobu, Nano Letters **12**, 4013 (2012).
[22] B. Radisavljevic, M. B. Whitwick, and A. Kis, ACS Nano **5**, 9934 (2011).
[23] H. Wang, L. L. Yu, Y. H. Lee, Y. M. Shi, A. Hsu, M. L. Chin, L. J. Li, M. Dubey, J. Kong, and T. Palacios, Nano Letters **12**, 4674 (2012).
[24] H. P. Komsa and A. V. Krasheninnikov, Physical Review B **91**, 125304 (2015).
[25] A. Kushima, X. F. Qian, P. Zhao, S. L. Zhang, and J. Li, Nano Letters **15**, 1302 (2015).
[26] P. Giannozzi, S. Baroni, N. Bonini, and *et al.*, Journal of Physics-Condensed Matter **21**, 395502 (2009).
[27] H.-P. Komsa, J. Kotakoski, S. Kurasch, O. Lehtinen, U. Kaiser, and A. V. Krasheninnikov, Phys. Rev. Lett. **109**, 035503 (2012).
[28] J. P. Perdew, K. Burke, and M. Ernzerhof, Phys. Rev. Lett. **77**, 3865 (1996).
[29] A. Ramasubramaniam, Physical Review B **86**, 115409 (2012).
[30] C. Freysoldt, J. Neugebauer, and C. G. Van de Walle, Physica Status Solidi B-Basic Solid State Physics **248**, 1067 (2011).
[31] C. Freysoldt, J. Neugebauer, and C. G. Van de Walle, Physical Review Letters **102**, 016402 (2009).
[32] Y. Kumagai and F. Oba, Physical Review B **89**, 195205 (2014).
[33] H.-P. Komsa, N. Berseneva, A. V. Krasheninnikov, and R. M. Nieminen, Phys. Rev. X **4**, 031044 (2014).
[34] D. Vinichenko, M. G. Sensoy, C. M. Friend, and E. Kaxiras, submitted.
[35] K. F. Mak, C. Lee, J. Hone, J. Shan, and T. F. Heinz, Physical Review Letters **105**, 136805 (2010).
[36] S. W. Han, G. B. Cha, E. Frantzeskakis, I. Razado-Colambo, J. Avila, Y. S. Park, D. Kim, J. Hwang, J. S. Kang, S. Ryu, W. S. Yun, S. C. Hong, and M. C. Asensio, Physical Review B **86**, 115105 (2012).
[37] A. Splendiani, L. Sun, Y. B. Zhang, T. S. Li, J. Kim, C. Y. Chim, G. Galli, and F. Wang, Nano Letters **10**, 1271 (2010).
[38] C. Lee, H. Yan, L. E. Brus, T. F. Heinz, J. Hone, and S. Ryu, ACS Nano **4**, 2695 (2010).
[39] A. R. Beal and H. P. Hughes, Journal of Physics C-Solid State Physics **12**, 881 (1979).
[40] Z. Y. Zhu, Y. C. Cheng, and U. Schwingenschlogl, Physical Review B **84**, 153402 (2011).
[41] H. P. Komsa and A. V. Krasheninnikov, Physical Review B **86**, 241201 (2012).
[42] S. Fang, R. Kuate Defo, S. N. Shirodkar, S. Lieu, G. A. Tritsaris, and E. Kaxiras, Phys. Rev. B **92**, 205108 (2015).
[43] P. Johari and V. B. Shenoy, ACS Nano **6**, 5449 (2012).
[44] S. Bertolazzi, J. Brivio, and A. Kis, ACS Nano **5**, 9703 (2011).
[45] T. J. Wieting and J. L. Verble, Physical Review B **3**, 4286 (1971).
[46] G. Henkelman, B. P. Uberuaga, and H. Jonsson, Journal of Chemical Physics **113**, 9901 (2000).
[47] H. P. Komsa, S. Kurasch, O. Lehtinen, U. Kaiser, and A. V. Krasheninnikov, Physical Review B **88**, 035301 (2013).
[48] S. S. Wang, G. D. Lee, S. Lee, E. Yoon, and J. H. Warner, ACS Nano **10**, 5419 (2016).
[49] F. Fabbri, E. Rotunno, E. Cinquanta, D. Kaplan, L. Lazzarini, M. Longo, A. Molle, V. Swaminathan, and G. Salviati, MRS Symposia Proceedings, Symposium EE, Fall Meeting (2015).
[50] F. Aryasetiawan and O. Gunnarsson, Reports on Progress in Physics **61**, 237 (1998).